Biosensors and Bioelectronics 54 (2014) 628–633

Contents lists available at ScienceDirect

Biosensors and Bioelectronics

journal homepage: www.elsevier.com/locate/bios

A novel electrochemical biosensor for monitoring protein nitration damage affected by $NaNO_2$/hemin/H_2O_2

Yanjuan Tang, Yanjie Guo, Lu Zhang, Jiye Cai, Peihui Yang *

Department of Chemistry, Jinan University, Guangzhou 510632, China

ARTICLE INFO

Article history:
Received 28 August 2013
Received in revised form
17 November 2013
Accepted 18 November 2013
Available online 27 November 2013

Keywords:
Protein nitration damage
$NO_2^{\bullet}$
Bovine serum albumin
$NaNO_2$/hemin/H_2O_2
Electrochemical biosensor

ABSTRACT

A sensitive and facile electrochemical biosensor has been developed for monitoring the protein nitration damage affected by the nitro free radicals($NO_2^{\bullet}$). The $NO_2^{\bullet}$ radicals is generated from hemin-catalyzed oxidation of nitrite (NO_2^-) in the presence of hydrogen peroxide (H_2O_2). In this work, nanocomposite films of graphene-gold nanoparticles (EG-AuNPs) were modified on the glassy carbon electrode by electropolymerization. Bovine serum albumin (BSA) was then further assembled on EG-AuNPs film through Au–S bond. The damage of BSA molecule was caused by the $NO_2^{\bullet}$ radicals which was generated from the $NaNO_2$/hemin/H_2O_2 nitration reagent. The differential pulse voltammetry was used to detect the damage of BSA molecule. Fluorescence spectra and circular dichroism spectrum further confirmed the nitration damage of BSA. Moreover, the lowest concentration at which the BSA damage was detected is 28.9 μM NO_2^- or H_2O_2, and the volume ratio of NO_2^- and H_2O_2 was 1:1 in the hemin/NO_2^-/H_2O_2 nitration reagent. The results demonstrated that the proposed electrochemical method can be used to detect protein damage affected by nitration reagent. The developed electrochemical biosensor is envisioned to have promising applications in protein damage studies.

1. Introduction

Reactive oxygen species (ROS) and reactive nitrogen species (RNS) are important groups of free radicals which are capable of eliciting direct damaging effects or acting as critical intermediate signaling molecules, leading to oxidative and nitrosative stress and a series of biological consequences(Helen Wiseman 1996). The $NO_2^{\bullet}$ radical as one kind of RNS, is a potent oxidant and nitrating agent. Excessive generating of $NO_2^{\bullet}$ radical can damage protein, DNA and polyunsaturated fatty acids, and may lead to oxidative stress and a variety of diseases. The nitration of proteins modulates catalytic activity, cell signaling, and cytoskeletal organization (Chiappetta et al., 2009; Darley-Usmar and Halliwell, 1996; Fang, 2004). Therefore, the study about nitration damage induced by $NO_2^{\bullet}$ radical on protein plays a crucial role in the study of biological toxicity and pathogenic mechanism of $NO_2^{\bullet}$ radical.

NO_2^- widely existed in plants, water and was one of the key sources of RNS. It is widely believed that $NO_2^{\bullet}$ radical can be generated by hemin peroxidase/H_2O_2/NO_2^- system in situ and induce the enzymatic nitration of various compounds including bio-macromolecules, where the peroxidase includes myeloperoxidase (MPO), lactoperoxidase, and horseradish peroxidase (HRP). The immunization, High Performance Liquid Chromatography (HPLC), capillary electrophoresis, and UV spectrophotometry are usually used to detect protein nitration damage induced by RNS (Shiraiwa et al., 2012; Tsai et al., 2011; Yuan et al., 2012; Zhang et al., 2012). For instance, Bian et al. explored the nitration damage of $NaNO_2$/hemin/H_2O_2 on protein by Western blot (Bian et al., 2003); Lu et al. confirmed the different effects of DFO on hemin/NO_2^-/H_2O_2-induced protein nitration and oxidation with UV–vis spectra and Western blotting (Lu et al., 2008). Lu et al. demonstrated that EDTA-Fe(III), ferric citrate, ferritin, and heme (hemin and hemoglobin) showed higher efficiency in catalyzing protein nitration in the NO_2^-/H_2O_2 system (Lu et al., 2011). These approaches have confirmed the nitration effect of $NaNO_2$/hemin/H_2O_2 on protein, which provide the detailed molecular information on protein damage. Unfortunately, most of them are either time-consuming and labor intensive or require highly technical expertise and relative sophisticated instrumentation. Therefore, it is necessary to build a new, facile and simple method to evaluate the protein nitration damage induced by hemin/NO_2^-/H_2O_2.

In recent years, electrochemical methods aroused increasing interest among researchers in detecting the nitration and oxidation damage with the benefits of being simple, rapid, and convenient. Bian et al. analyzed Fenton-mediated oxidative damage on BSA using poly-o-phenylenediamine as electroactive probe (Bian et al., 2011). Wang showed a novel biosensor for the study of BSA damage induced by Fenton reaction using tris-(2,2-bipyridyl)

* Corresponding author. Tel./fax: +86 20 85221679.
E-mail addresses: stangyanjuan@126.com (Y. Tang), 380442985@qq.com (Y. Guo), 315653534@qq.com (L. Zhang), tjycai@jnu.edu.cn (J. Cai), typh@jnu.edu.cn (P. Yang).

0956-5663/$ - see front matter © 2013 Elsevier B.V. All rights reserved.
http://dx.doi.org/10.1016/j.bios.2013.11.052

cobalt(III) perchlorate as the electroactive indicator (Wang et al., 2012). Zhang et al. developed a novel electrochemical platform for detection of the DNA damage induced by the NO_2^-/H_2O_2 system (Zhang et al., 2012). To date, a few studies on using the electrochemical method for the detection of protein oxidation damage have been reported. However, there have been few reports concerning the electrochemical sensing of protein nitration damage induced by hemin/NO_2^-/H_2O_2.

Graphene has recently attracted great attention due to its unique electrical, optical, and mechanical properties as well as its potential use in various fields, such as electronics, supercapacitors, sensors, and composite materials. Liu et al. have reported a simple method for the synthesis of graphene-AuNPs nanocomposite films by using a coelectrodeposition technique (Liu et al., 2011). The proposed EG-AuNPs exhibited better conductivity, larger surface area and better biocompatibility compared to the pure graphene film. Therefore, this can establish a foundation for fabricating electrochemical biosensor to detect protein nitration damage induced by $NO_2^{\bullet}$ radical.

Herein, protein nitration damage was investigated for the first time by the electrochemical method based on the attenuation of conductivity after damage caused by $NO_2^{\bullet}$ radical. Oxidation signal of $[Fe(CN)_6]^{4-/3-}$ was used as an indicator for the sensitive detection of BSA damage based on evidently attenuation of conductivity. The detecting mechanism of the exhibited electrochemical biosensor was shown in Scheme 1. GO–$HAuCl_4$ mixed solution can be direct reduced to yield EG-AuNPs nanocomposites on the electrode surface by electrodeposition. BSA was modified on EG-AuNPs composite film by Au–S bond. The $NO_2^{\bullet}$ radical produced by the $NaNO_2$/hemin/H_2O_2 system can induce the damage of protein, which could change the electroactivity of protein interface and realize the monitoring of the protein nitration damage. The nitration mechanism of hemin/NO_2^-/H_2O_2 on protein was as follows (Radi 2004, 2012):

$$Hemin(Fe^{3+}) + H_2O_2 \rightarrow Hemin^{\bullet\pi+}(Fe^{4+}) \quad (compound1) \qquad (1)$$

$$Hemin^{\bullet\pi+}(Fe^{4+}) + NO_2^- \rightarrow Hemin(Fe^{4+}) + NO_2^{\bullet} k \quad (compound2) \qquad (2)$$

$$Hemin(Fe^{4+}) + NO_2^- \rightarrow Hemin(Fe^{3+}) + NO_2 \qquad (3)$$

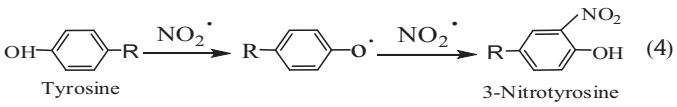

(4)

2. Experimental

2.1. Chemicals and reagents

AnnexinV (35–36 kDa), hemoglobin and bovine serum albumin (BSA) were purchased from Boisynthesis Biotechnology Co., Ltd. (Beijing, China) and used without further purification. Ascorbic acid, chlorogenic acid and resveratrol (RVL) were purchased from Lang Ze Pharmaceutical Technology Co., Ltd. (Nanjing, China). L-Tyrosine was purchased from Guangzhou Chemical Reagent Co. (Guangzhou, China). All other reagents were of analytical reagent grade. Double-distilled water was used in all experiments.

2.2. Apparatus

Electrochemical measurements were performed by a model CHI660A electrochemical workstation (CH Instruments, Chenhua Co., Shanghai, China). A three-electrode system was used in the measurements, with a bare GCE(4 mm in diameter) or nanobiocomposite film modified GCE as the working electrode, a saturated calomel electrode (SCE) as the reference electrode and a platinum foil as the auxiliary electrode. differential pulse voltammetry (DPV) and cyclic votammetry (CV) were used to make electrochemical measurements. The conditions of DPV were as follows: pulse amplitude 50 mV, and pulse period 0.5 s. The scan potential range was from 0 to 0.8 V (vs. SCE) in the present of 10 mM $[Fe(CN)_6]^{3-/4-}$ solution containing 0.1 M KCl. CV measurement was performed at scan rate of 0.1 V/s. Photoluminescence (PL) spectrum was performed on a 970CRT fluorescence spectrophotometer (Shanghai, China). The structure of protein was characterized by circular dichroism spectrum (CD spectra) (Applied Photophysics Ltd., England).

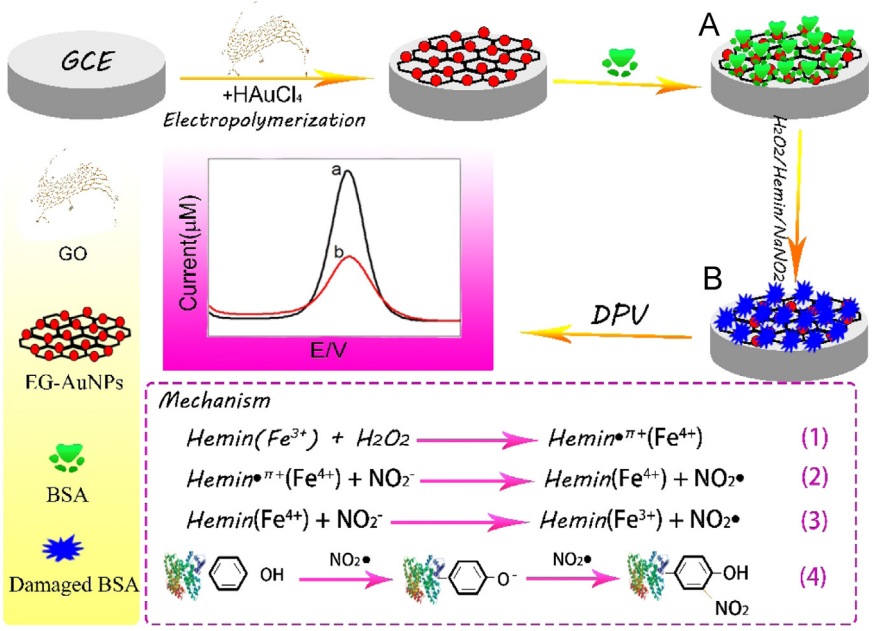

Scheme 1. Schematic diagram of BSA nitration damage induced by $NaNO_2$/hemin/H_2O_2.

2.3. Construction of GCE/EG-AuNPs/BSA

Graphite oxide was prepared from natural graphite by a modified Hummers' method (Hummers and Offeman 1958). The synthesized graphite oxide powder was exfoliated in electrolytes by ultra-sonication for 30 min to form homogeneous GO dispersions with a concentration of 1.0 mg mL^{-1}. The graphene-AuNPs composites were electrodeposited in situ on the GCE surface according to the reported method (Liu et al., 2011). The bare GCE electrode was polished sufficiently with 0.05 μm alumina slurry, followed by successive sonication in both ethanol and double distilled water for 5 min. Then, the electrode was dipped in the dispersion containing 1.0 mg mL^{-1} GO and 100 μM tetrachloroauric acid ($HAuCl_4$), and cyclic voltammetry (CV) was performed between −1.5 and +0.6 V (vs. SCE) for the potential scanning of 10 cycles. The EG-AuNPs modified electrode was washed with doubly distilled water and then immersed in BSA solution for 2 h at room temperature. Finally, the electrode surface was rinsed with 0.1 M PBS buffer to remove the nonspecifically absorbed species.

2.4. Effects of biosensor and $NaNO_2$/hemin/H_2O_2 nitration reagent

Scheme 1 shows the detection mechanism of BSA damage induced by $NO_2^{\bullet}$ radical. Biosensor response was obtained by DPV before incubation. Then the modified electrodes were incubated in pH 7.4 PBS containing 25 μM hemin, 1 mM $NaNO_2$ and 1 mM H_2O_2 (the nitration reagent) for 1 h, followed by washing and subsequent DPV analysis. During the course of the incubation treatment in the cleavage agent, hemin, $NaNO_2$ and H_2O_2 reacted to produce $NO_2^{\bullet}$, $NO_2^{\bullet}$ attacked the BSA film and induced BSA damage. The DPV peak current difference of the $[Fe(CN)_6]^{3-/4-}$ probe after and before incubation in the nitration reagent was used as the measurement signal for BSA damage. Considering the variation for replicative electrode, the relative peak current ratio (I/I_0), instead of absolute peak current, was used to evaluate the effect of BSA damage, where I_0 and I represent the DPV peak current for the films before and after incubated in the nitration reagent, respectively. The dependence of damage degree on the concentration of BSA, the contents of the nitration reagent, and incubation time are described in Fig. 2.

3. Results and discussion

3.1. Electrochemical behaviors of GCE/EG-AuNPs/BSA

Nanocomposite films of GCE/EG-AuNPs/BSA were characterized by differential pulse voltammetry (Fig. 1). The DPV signals of BSA nitration damage were detected after incubation with the nitration reagent for 60 min using $Fe(CN)_6^{4-/3-}$ as electroactive probes. The DPV signal decreased as BSA was immobilized on the GCE/EG-AuNPs surface. When BSA was damaged by $NO_2^{\bullet}$ radical, the DPV signal further decreased, which was due to evidently attenuation of biosensor conductivity. However, there was no redox signals after incubation with $NO_2^{\bullet}$ radical in the control solution in the absence of $Fe(CN)_6^{4-/3-}$ probes. The result indicated that the proposed biosensor could sensitively detect the damage of BSA. The more detailed mechanism needs further research.

3.2. Optimization of the experimental conditions

The amount of BSA immobilized on the surface of GCE/EG-Au/BSA electrode is an important factor for the detection of BSA damage. As shown in Fig. 2A, a sharp decrease of DPV signal is observed with the increasing concentration of BSA. Then it tended

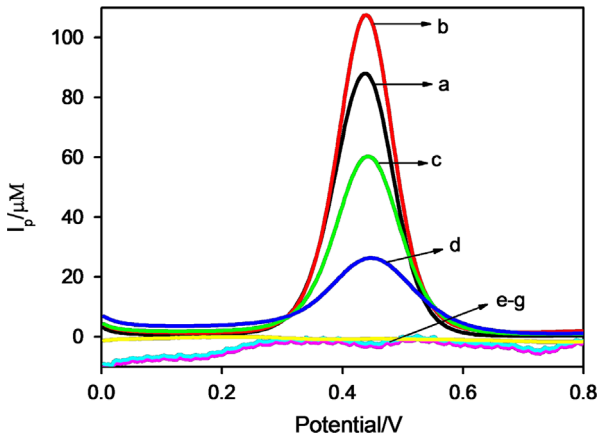

Fig. 1. DPVs in 0.1 M $K_3Fe(CN)_6/K_4Fe(CN)_6$ (0.1 M KCl) of GCE (a), GCE/EG-AuNPs (b), GCE/EG-AuNPs/BSA before (c) and after (d) incubation with 1 mM $NaNO_2$, 25 μM hemin and 1 mM H_2O_2 for 60 min. DPVs in 0.1 PBS (pH 7.4) of GCE/EG-AuNPs, GCE/EG-AuNPs/BSA before and after incubation with 1 mM $NaNO_2$, 25 μM hemin and 1 mM H_2O_2 for 60 min (e–g).

to a steady value as the concentration of BSA was more than 0.6 mg/mL, indicating a saturated surface density to thoroughly damaged BSA. Another significant factor for detecting the BSA damage is the nitration time. The DPV signal decreased with the increasing nitration time in the solution containing 25 μM hemin, 1 mM $NaNO_2$ and 1 mM H_2O_2, and then the DPV signal reached a plateau at 60 min (Fig. 2B). Meanwhile, when BSA modified biosensor was incubated with the nitration reagent in pH 7.4 PBS buffer solution, the value of I/I_0 decreased rapidly for the first 20 min, indicating that the damage process in hemin/NO_2^-/H_2O_2 reagents carried through at a fast rate.

There was no influence on the current response as H_2O_2, $NaNO_2$ or hemin were used as blank, but the peak current decreased apparently in the presence of nitration reagent (Fig. 2C). It showed that BSA was damaged in the nitration reagent solution with NO_2^- and H_2O_2 (the volume ratio=1:1). The peak current shown in Fig. 2D was proportional to the logarithmic value of the concentration of NO_2^- or H_2O_2 in the range of 0.05 to 2 mM. The linear regression equation was $I = -0.97636 - 0.25939\log C_{H_2O_2}$ with a correlation coefficient R of 0.9913. The lowest concentration at which the BSA damage was detected could be 28.9 μM NO_2^- or H_2O_2, and it was estimated from the formula $I_{LOD} = I_{control} + 3I_{stdev\ (con)}$, where $I_{control}$ was the peak current in the absence of the hemin/NO_2^-/H_2O_2 system and $I_{stdev(con)}$ represented the standard deviation of $I_{control}$. From the above experiments, it can be concluded that BSA damage was caused by $NO_2^{\bullet}$ radical and the proposed method can be used for the determination of BSA damage expediently.

3.3. Validation of BSA damage

Cyclic voltammetry (CV) is a facile electrochemical technique to investigate the interface properties of chemically modified electrode surface. Fig. 3A displays the CV curves of different electrodes in the presence of 0.1 M $[Fe(CN)_6]^{4-/3-}$ solution. It is clear that the current response of the BSA molecule modified electrode decreased obviously after incubation with nitration reagent. Apparently decrease in peak current after damage is mainly due to changes in protein conformation induced by $NO_2^{\bullet}$ radical making the BSA film less porous, and the changes of protein conformation could further prevent the transfer of electron to the electrode surface. Here, the changes of protein conformation and damage sites of BSA molecule were characterized by CD spectrum and fluorescence spectrum.

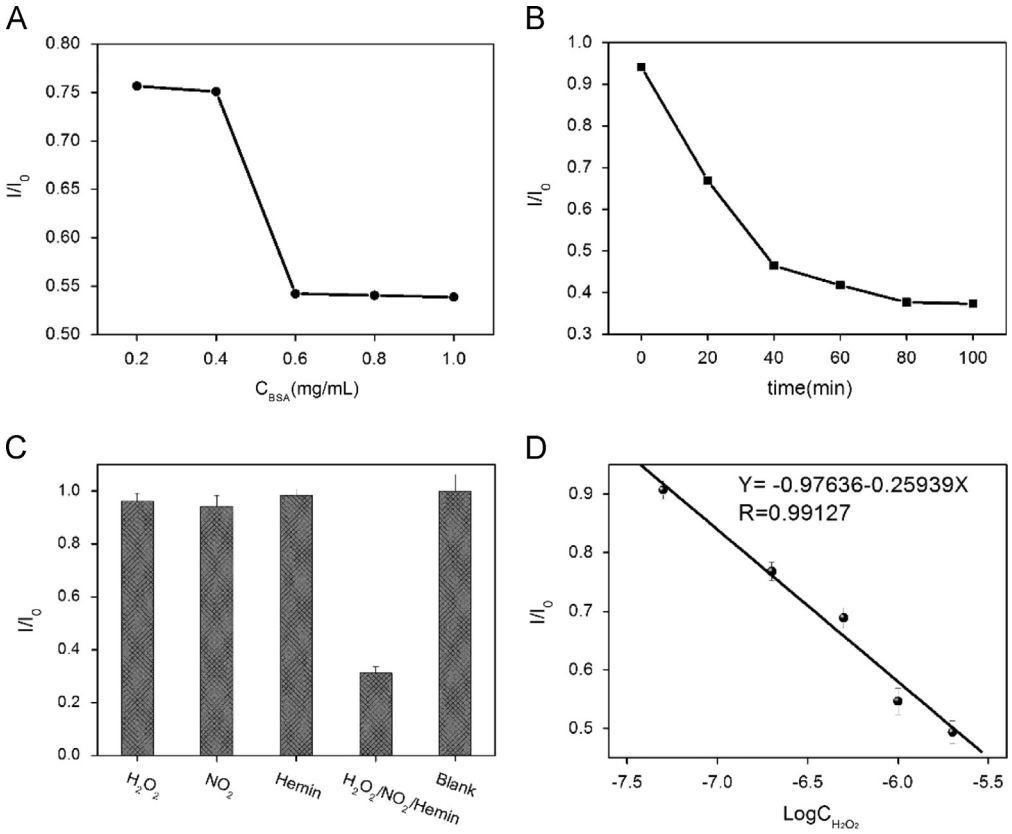

Fig. 2. Dependence of DPV peak current ratio I/I_0 for BSA film in 0.1 M $K_3Fe(CN)_6/K_4Fe(CN)_6$ (0.1 M KCl). (A) After incubating with the concentration of BSA in the range of 0.2–1.0 mg/mL. (B) On the incubation time in pH 7.4 PBS containing 1 mM $NaNO_2$, 25 μM hemin and 1 mM H_2O_2. (C) Dependence of DPV oxidative peak current ratio I/I_0 for BSA film after incubating with $NaNO_2$/hemin/H_2O_2 reagents or control solutions. (D) The plot of I/I_0 vs. log $C_{H_2O_2}$.

Exposure of proteins to $NO_2^{\bullet}$ radical leads to gross structural modifications. The CD spectrum can be used to monitor changes in protein conformation (Greenfield, 2007). Fig. 3B shows the CD spectra of BSA before and after incubation with the nitration reagent. The spectra of BSA have features that are characteristic of an α-helical structure, minima at 222 and 208 nm and a maximum at around 192 nm (Kelly and Price, 2000). From this spectra, we could obviously see changes at 222, 208 and 192 nm, which indicated $NO_2^{\bullet}$ radical affected the secondary structure of BSA. This result was according with the previous report that nitration site of protein occurred in the structure of α-helical and β-sheet. The CD spectrum confirmed that nitration reagent could induce BSA damage.

Fluorescence spectrum is a classical approach for detecting the changes of protein residue. It is well known that the fluorescence of BSA results from the tyrosine, tryptophan and phenylalanine residues. From Fig. 3C, it could be seen that BSA had a fluorescence emission peak at 351 nm with excitation wavelength of 280 nm; whereas nitration reagent had no intrinsic fluorescence. The fluorescence intensity of BSA could be quenched by nitration reagent, and gradually decreased with the increasing concentration of nitration reagent, which indicated that nitration reagent could cause the changes of protein conformation.

To further confirm the damage site of BSA which was mainly occurred in tyrosine residue, we observed the fluorescence intensity changes of L-tyrosine after incubation with nitration reagent. Fig. 3D showed that L-tyrosine had a obvious fluorescence peak at 303 nm with excitation wavelength of 280 nm. After treatment with the nitration reagent, the fluorescence intensity of L-tyrosine obviously decreased, which demonstrated that $NO_2^{\bullet}$ radical could damage tyrosine residue. Therefore, the results provided the strong evidence that peak current decrease of BSA film on electrode surface was due to the changes in protein conformation induced by $NO_2^{\bullet}$ radical.

3.4. Selectivity of hemin/H_2O_2/$NaNO_2$ on protein damage

In recent years, the mechanism of protein damage site induced by $NO_2^{\bullet}$ radical is a hot issue. There existed selectivity and specificity of the nitration reagent on protein damage. To explore the factors of the nitration reagent on protein damage, we used the proposed biosensor to monitor the nitration degree for the nitration reagent on different types of proteins. Fig. 4 showed the nitration degree of the nitration reagent on BSA, hemoglobin and annexinV. We could see ΔI_{BSA} is smaller than $\Delta I_{Hemoglobin}$ and $\Delta I_{annexinV,}$ which indicating that the nitration degree of the nitration reagent on BSA is lower than that on hemoglobin and annexinV. Although there is no obvious difference in molecular weight between BSA and hemoglobin, and they all present the spherical secondary structure which makes tyrosine residue pack in protein. While hemoglobin has a ferrous ion which could catalyze protein nitration. In addition, compared with BSA and hemoglobin, annexinV has smaller molecular weight, and tyrosine residue is exposed on the surface of protein. Herein, the more exposal degree of tyrosine residue on the surface of protein and the more amount of iron in protein, the bigger the nitration degree of the nitration reagent on protein is. Most importantly, the variation tendency of the proposed method matched that from the fluorescence spectroscopic method, which strongly evidenced that the proposed method could effectively detect the nitration effect of the nitration reagent on proteins.

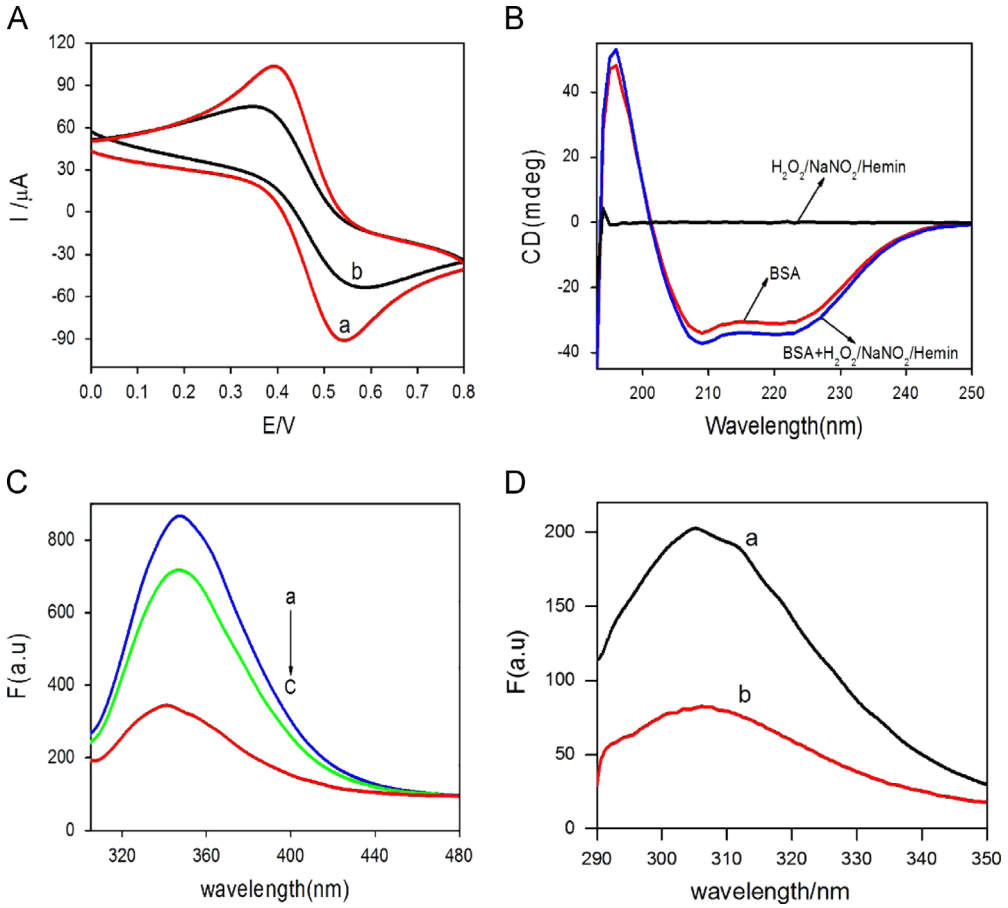

Fig. 3. (A) CVs of GCE/EG-AuNPs/BSA in 0.1 M $K_3Fe(CN)_6/K_4Fe(CN)_6$ (0.1 M KCl) before and after incubation with 1 mM $NaNO_2$, 25 μM hemin and 1 mM H_2O_2 for 60 min. (B) The CD spectrum of BSA before and after incubation with 1 mM $NaNO_2$, 25 μM hemin and 1 mM H_2O_2 for 60 min. (C) The fluorescence spectra of BSA before and after incubation with 1 mM $NaNO_2$, 25 μM hemin, 1 mM H_2O_2 and 0.5 mM$NaNO_2$, 12.5 μM hemin, 0.5 mM H_2O_2 for 60 min. (D) The fluorescence spectra of L-tyrosine before and after incubation with 1 mM $NaNO_2$, 25 μM hemin and 1 mM H_2O_2 for 60 min.

3.5. Protection effect of antioxidants to BSA

Several small molecule antioxidants including ascorbic acid (AA), chlorogenic acid, resveratrol (RVL) and others were reported to be excellent free radical scavengers (Chen et al., 2013; Guo et al., 2007; Perron et al., 2008). Here, antioxidants were used to scavenge the nitro free radicals ($NO_2^{\bullet}$) produced by the nitration reagent, which further proved the protective effect of antioxidants on BSA. Table 1 indicated that the half maximal effective concentration (EC_{50}) were 91.97 μM ± 0.03, 41.66 μM ± 0.02 and 23.96 μM ± 0.02 for AA, chlorogenic acid and RVL, respectively. The result revealed that these three antioxidants have the well scavenging ability on the nitro free radicals ($NO_2^{\bullet}$), which directly proved the protection effect of antioxidants on BSA and sufficiently evidenced the feasibility of the established method.

3.6. Stability and reproducibility

Stability and fabrication reproducibility were important parameters for the proposed biosensor. Generally, GCE/EG-AuNPs/BSA electrode can be kept stable for 10 days under the anaerobic condition. For 10 successive determinations at the same biosensor, the relative standard deviation (R.S.D) was 2.95%. Fabrication reproducibility was estimated with five different electrodes, which were constructed by the same procedure, and the R.S.D was 2.05%. As a result, the proposed biosensor exhibited comparative stability and good reproducibility.

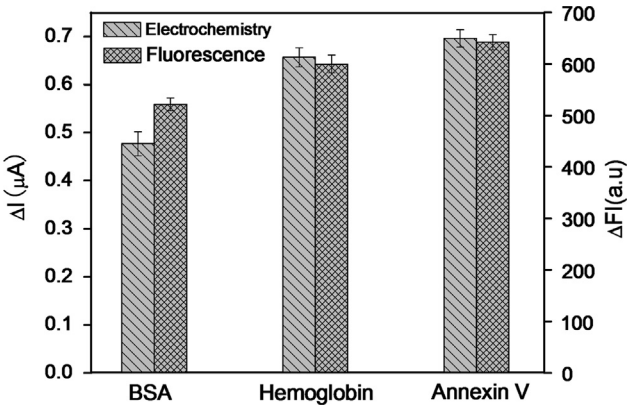

Fig. 4. Δ*I* and Δ*FI* of BSA, hemoglobin and annexinV after incubating with 1 mM $NaNO_2$, 25 μM hemin and 1 mM H_2O_2 for 60 min.

4. Conclusions

In conclusion, a novel GCE/EG-AuNPs/BSA electrochemical biosensor was explored to evaluate the protein nitration damage affected by $NO_2^{\bullet}$ radical produced from hemin/H_2O_2/$NaNO_2$ nitration reagent. The nitration damage of BSA was detected by differential pulse voltammetry and the peak currents decreased obviously due to changes in protein conformation making the BSA film less porous. The BSA damage was also validated by fluorescence spectra and CD spectra. Meanwhile, some typical

Table 1
EC_{50} of antioxidants.

Antioxidants	Half-inhibition concentration (EC_{50}) (μM)
Ascorbic acid	91.97 ± 0.03
Chlorogenic	41.66 ± 0.02
Resveratrol	23.96 ± 0.02

Values are the means of three replicates ± SD.

antioxidants such as AA, chlorogenic acid and RVL were used to eliminate the nitro free radicals, which directly confirmed the nitration effect of nitrating agent to BSA and further verified the feasibility of the proposed method. This strategy provided a simple, sensitive, stable analytical method for the detection of protein damage induced by nitrating agent.

Acknowledgments

This work was supported by the grants from National Natural Science Foundation of China (Nos. 21071064 and 21375048). The Major State Basic Research Development Program of China (973 Program) (No. 2010CB833603).

References

Bian, C., Xiong, H., Zhang, X., Wen, W., Wang, S., 2011. Biosens. Bioelectron. 28, 216–220.
Bian, K., Gao, Z., Weisbrodt, N., Murad, F., 2003. Proc. Natl. Acad. Sci. 100, 5712–5717.
Chen, L., Wu, N., Sun, B., Su, H., Ai, S., 2013. Microchim. Acta. 180, 573–580.
Chiappetta, G., Corbo, C., Palmese, A., Marino, G., Amoresano, A., 2009. Proteomics 9, 1524–1537.
Darley-Usmar, V., Halliwell, B., 1996. Pharm. Res. 13, 649–662.
Fang, F.C., 2004. Nat. Rev. Microbiol. 2, 820–832.
Greenfield, N.J., 2007. Nat. Protoc. 1, 2527–2535.
Guo, S., Deng, Q., Xiao, J., Xie, B., Sun, Z., 2007. J. Agric. Food Chem. 55, 3134–3140.
Helen Wiseman, Barry Halliwell., 1996. Biochem. J. 313, 17–29.
Hummers, W.S., Offeman, R.E., 1958. J. Am. Chem. Soc. 80, 1339.
Kelly, S.M., Price, N.C., 2000. Curr. Protein Pept. Sci. 1, 349–384.
Liu, C., Wang, K., Luo, S., Tang, Y., Chen, L., 2011. Small. 7, 1203–1206.
Lu, N., Li, X., Li, J., Xu, W., Li, H., Gao, Z., 2011. J. Biol. Inorg. Chem. 16, 481–490.
Lu, N., Zhang, M., Li, H., Gao, Z., 2008. Chem. Res. Toxicol. 21, 1229–1234.
Perron, N.R., Hodges, J.N., Jenkins, M., Brumaghim, J.L., 2008. Inorg. Chem. 47, 6153–6161.
Radi, R., 2004. Proc. Natl. Acad. Sci. 101, 4003–4008.
Radi, R., 2012. Accounts Chem. Res. 46, 550–559.
Shiraiwa, M., Selzle, K., Yang, H., Sosedova, Y., Ammann, M., Pöschl, U., 2012. Environ. Sci. Technol. 46, 6672–6680.
Tsai, Y.-C., Wang, Y.-H., Liou, C.-C., Lin, Y.-C., Huang, H., Liu, Y.-C., 2011. Chem. Res. Toxicol. 25, 191–196.
Wang, Y., Xiong, H., Zhang, X., Wang, S., 2012. Electrochim. Acta 67, 147–151.
Yuan, C., Li, H., Gao, Z., 2012. J. Biol. Inorg. Chem. 17, 1083–1091.
Zhang, Y., Liu, H., Hu, N., 2012. Bioelectrochemistry. 86, 67–71.